

ELEVATING THERMOELECTRIC PERFORMANCE OF ORGANIC COMPOSITES VIA HIERARCHICAL NANOSTRUCTURE INTEGRATION

Mahesh Kumar Chandna

Research Scholar

Physics

Dr. Vivek Yadav

(Associate Professor)

Department of Science, Sunrise University Alwar

DECLARATION: I AS AN AUTHOR OF THIS PAPER /ARTICLE, HERE BY DECLARE THAT THE PAPER SUBMITTED BY ME FOR PUBLICATION IN THE JOURNAL IS COMPLETELY MY OWN GENUINE PAPER. IF ANY ISSUE REGARDING COPYRIGHT/PATENT/ OTHER REAL AUTHOR ARISES, THE PUBLISHER WILL NOT BE LEGALLY RESPONSIBLE. IF ANY OF SUCH MATTERS OCCUR PUBLISHER MAY REMOVE MY CONTENT FROM THE JOURNAL WEBSITE. FOR THE REASON OF CONTENT AMENDMENT /OR ANY TECHNICAL ISSUE WITH NO VISIBILITY ON WEBSITE /UPDATES, I HAVE RESUBMITTED THIS PAPER FOR THE PUBLICATION. FOR ANY PUBLICATION MATTERS OR ANY INFORMATION INTENTIONALLY HIDDEN BY ME OR OTHERWISE, I SHALL BE LEGALLY RESPONSIBLE. (COMPLETE DECLARATION OF THE AUTHOR AT THE LAST PAGE OF THIS PAPER /ARTICLE)

ABSTRACT

A comprehensive system architecture suggested integrating hierarchical nanostructures to increase the thermoelectric productivity of organic composites. The review delves into the multi-layered strategy of employing hierarchical nanostructures, including Nano organizing, interfacial designing, and dopant consolidation, to simultaneously improve the electrical conductivity, Seebeck coefficient, and warm conductivity, with a focus on the burgeoning field of organic thermoelectric materials. In the most recent advancements in nanomaterial science and nanotechnology development, hierarchical nanostructure—a created nanostructure with a larger get together degree of constituents by low layered Nano-building blocks—has received considerable attention. The ordered hierarchical nanostructures may have advantages such as more dynamic locations, synergistic qualities deduced from their mathematical complexity and diversity of construction elements, and the resulting multifunctionalities. Because of their easy handling, low material overflow, and earth-harmless characteristics, organic thermoelectric (TE) materials are quite attractive. However, their actual potential is severely constrained by their poor thermoelectric capabilities. In this work, poly(3,4-ethylenedioxythiophene) poly(styrene sulfonate) was combined by covalently functionalizing graphene with fullerene via p stacking in a liquid mark of connection. While fullerene expands the Seebeck coefficient and decreases warm

conductivity, graphene assists with working on electrical conductivity. This outcomes in a synergistic impact that upgrades thermoelectric qualities.

Keywords: *Elevating, Thermoelectric Performance, Organic Composites, VIA, Hierarchical Nanostructure, Integration*

1. INTRODUCTION

Thermoelectric materials have an exceptional ability to change over squander heat into power, giving a reasonable answer for energy assortment and usage. As a result of their innate flexibility, minimal expense, and simplicity of dealing with, organic composites have arisen as an especially intriguing class among the different materials read up for thermoelectric applications. Nonetheless, their moderately humble thermoelectric performance has restricted their viable execution. Examiners have been effectively exploring techniques to improve the thermoelectric qualities of organic composites to meet this test. Utilizing hierarchical nanostructures is one methodology that shows guarantee for controlling charge and phonon transport at various length scales and expanding the thermoelectric efficiency of these materials.

From the Nano meter to the miniature meter scale, hierarchical nanostructures cover a great many components and give exact command over material performance and characteristics. By lessening dispersal and further developing carrier transport courses, the consolidation of nanoparticles or nanofibers into organic structures can essentially upgrade the portability of charge carriers at the nanoscale. Additionally, Nano association lessens electrical opposition, propels effective charge transport, and increments surface region. Moreover, at the microscale, the consolidation of these nanostructures into wanted models — like porous plans or nanowire networks — empowers the guideline of phonon transport, which is significant for decreasing warm conductivity and raising the thermoelectric figure of authenticity, or ZT.

Contrasted with customary methods, the joining of hierarchical nanostructures into organic composites enjoys a couple of benefits. Fundamentally, it works with the unraveling of contradicting qualities like electrical and warm conductivity, permitting unlimited advancement towards upgrading thermoelectric productivity. Moreover, the capacity to change the shape and association of nanostructures assists with bettering adjust and stay

significant in different workplaces by matching the material's characteristics to explicit application necessities. Additionally, flexible and sharp techniques can be utilized to consolidate hierarchical nanostructures, guaranteeing the feasibility of colossal extension development for organization course of action.

Various methods, like real smoke declaration and manufactured smolder explanation systems, as well as plan based cycles, for example, electrospinning, self-social occasion, and design supported mix, have been created to deliver hierarchical nanostructures in organic composites. As to over the morphology of the nanostructure, flexibility, and similarity with various organic network materials, every one of the strategies give remarkable benefits. Besides, the fitting determination of nanostructure parts, for example, carbon-based materials, driving polymers, and inorganic nanoparticles, empowers the alignment of material properties to accomplish ideal thermoelectric performance.

Counting hierarchical nanostructures may up another road to work on organic composites' thermoelectric performance. Through the usage of the integral impacts of nanoscale configuration on charge and phonon transport, hierarchical nanostructured materials give improved proficiency, flexibility, and versatility for different thermoelectric purposes. Research in this space can possibly make new roads for down to earth energy collecting and application, propelling the production of best in class thermoelectric developments.

2. LITERATURE REVIEW

The connection between human development and energy utilization is examined by Akizu-Gardoki et al. (2018), who center around the idea of decoupling inside impression bookkeeping. The examination examines how human development, frequently estimated utilizing pointers, for example, the Human Development Index (HDI), can be accomplished without an equivalent expansion in energy use. The writers examine the normal impact of human action, especially concerning energy usage, utilizing impression accounting strategies. Through their examination, they distinguish cases of decoupling, in which headways in human development are not matched by a similar expansion in energy use. This revelation is huge for feasible development since it proposes that social headway can be made with less of an effect on the climate. The audit stresses that it is so vital to take on reasonable ways of

behaving and moves toward that reinforce decoupling to alleviate the environmental impacts of human action.

Balcilar et al. (2018) center around a gathering of G-7 nations to additional the writing on the complex connection between carbon dioxide fluxes, energy utilization, and financial development. The examination unravels the responsibilities of energy utilization and monetary factors to carbon dioxide emanations over the long run utilizing genuine corruption investigation. The creators give exact proof of the connection between these factors by examining the genuine examples, which reveals insight into the systems that drive the development of petroleum derivative squanders in present day economies. Their discoveries give experiences into the exchange between energy utilization and financial development, including the requirement for arrangements that advance feasible energy rehearses to lessen the side-effects of petroleum products and advance monetary development. The audit's emphasis on certifiable weakening adds subtlety to how we might interpret the complex examples found in petroleum derivative squanders and their essential causes.

Chu et al. (2017) center around mechanical degrees of progress and methodology drives in their thorough outline of the excursion towards supportable energy. To progress to a controllable energy structure, the exposition takes a gander at a few environmentally well disposed power sources, energy limit game plans, and efficiency increments. Using goodies of data from the field of materials science, the creators feature the job that original materials play in propelling energy advances like sunlight based cells and batteries. The evaluation additionally stresses the need of global collaboration and interdisciplinary composed exertion in tending to the difficulties of reasonable energy headway. The originators give a manual for policymakers, researchers, and industry accomplices chasing after a more possible energy future by enlightening significant methodologies and mechanical progressions. The careful way to deal with viable energy in the paper underlines the requirement for facilitated plans that take social, financial, and ecological variables into account.

Du et al. (2012) center around improving the thermoelectric qualities of a nanocomposite that contains graphene nanosheets and polyaniline (PANI). It is basic to involve thermoelectric materials to change over squander heat into power for use in energy gathering and gadget cooling. The creators present a clever way to deal with tending to the conductivity and

Seebeck coefficient of the nanocomposite, two basic boundaries impacting its thermoelectric performance. Through the integration of graphene nanosheets into the PANI organization, they accomplish common advantages that outcome in upgraded electrical conductivity and thermoelectric performance. By giving goodies of data about the plan and creation of nanocomposites with improved performance, this work progresses the field of thermoelectric materials and makes ready for more compelling energy change advancements.

To offer hydrogen as the ideal fuel, Duan et al. (2017) examine the electrocatalytic qualities of ultrathin metal-organic construction (MOF) bunches for water parting. The survey centers around the production of compelling impetuses for the principal steps in water parting, the hydrogen evolution reaction (HER) and oxygen evolution reaction (OER). The huge surface region and uncovered powerful areas of the force permit the makers to accomplish high reactant development and sufficiency through the creation of ultrathin MOF exhibits. The discoveries feature the capability of MOF-based materials for economical power applications, especially in the creation of hydrogen for energy capacity frameworks and power gadgets. This study propels the study of electrocatalysis by giving a flexible and compelling strategy for parting water, tending to difficulties in functional energy change.

In their 2013 review, He and partners explored the utilization of carbon-exemplified iron oxide (Fe_3O_4) nanoparticles as an anode material for lithium-molecule batteries. Their objective was to further develop battery performance, especially as to high-rate limit. The requirement for superior performance terminal materials is powered by the need of lithium-molecule batteries for electric vehicles and versatile equipment. The examination exhibits how the expansion of carbon exemplification works on the security and conductivity of Fe_3O_4 nanoparticles, empowering fast scattering of lithium particles and high-rate charge/discharge cycling. The creators accomplish unrivalled electrochemical performance by working on the association cycle and nanostructure plan. This could prompt the development of cutting-edge lithium-molecule batteries with further developed energy thickness and cycling strength. This exploration adds to the progression of cutting-edge terminal materials for lithium-molecule batteries, tending to the developing requirement for energy limit arrangements across a few enterprises.

3. METHODS AND MATERIALS

Asbury Carbons benevolently gave graphite. We utilized fullerene (98%, Sigma Aldrich) minus any additional refining. The accompanying things were bought from Sigma Aldrich: sodium chloride (practically 100 percent), N, N Dimethylformamide (DMF, anhydrous, 99.8%), phenylhydrazine (97%), isopropyl alcohol (IPA, 99.7%), and m-xylene (anhydrous, 99.9%). The ACS reagent, nitric destructive (seething), was bought from Across Organics. PEDOT: Clevios was the wellspring of PSS (PH 1000).

3.1.Preparation of graphite oxide.

Stripped graphite oxide had a material drop that came about in graphene. A changed form of Brodie's cycle delivered graphite oxide⁵⁵. Normally, room temperature was utilized to consolidate graphite (10 g), bubbling nitric corrosive (160 ml), and sodium chlorate (85 g), however this was managed without the ensuing development that Brodie's strategy calls for. As indicated by what Brodie depicted, the mixture was mixed for an entire day prior to being washed, sifted, and cleaned. Graphite oxide was gotten by scattering the game plan and utilizing a precipitation strategy.

3.2.Preparation of chemically reduced graphene oxide (rGO).

By diminishing graphite oxide with phenylhydrazine, graphene nanosheets were delivered. Ordinarily, 20 ml DMF was exposed to tip sonication at 50 W (Misonixsonicator 3000) for an hour to scatter 200 mg of graphite oxide and produce shed graphene oxide. Next, 0.5 ml of 35 weight percent phenylhydrazine from Sigma-Aldrich was added. The mixture was consolidated for 24 hours at room temperature, and afterward it was independently washed with 500 ml of DMF and 500 ml of ethanol. Present moment separating and treating of the materials at 270 uC in a vacuum oven brought about a diminishing in graphene.

3.3.Preparation of C60/rGO nanohybrids.

The C60/rGO nanohybrids were gathered at the liquid coupling point via p arrangement. Ordinarily, ultrasonication was utilized to scatter C60 and rGO in discrete m-xylene and IPA arrangements. By then, the C60/m-xylene game plan was continuously mixed with the rGO/IPA (500 mg/l) course of action at a volume proportion of 151. When two game plans were associated, the associated point of communication's shade turned dull green, demonstrating that rGO and C60 had hybridized. Subsequently, the interfacial suspension

was partitioned and moved with a needle into another estimating glass at regular intervals. Five distinct C60/m-xylene course of action fixations (0.1, 0.5, 0.75, 1 and 2 mg/ml) were utilized.

3.4.Preparation of C60/rGO-polymer composites.

After cautiously consolidating disengaged C60/rGO nanohybrids with PEDOT: PSS and present moment drying at 50 uC, the C60/rGO-polymer composite was ready. The weight proportion of PEDOT: PSS to hybridized nanohybrids was 357. The nanohybrid's fullerene to rGO proportion was 159, 357, 555, 852, 951; the examples were recognized as S1, S2, S3, S4, and S5, in a specific order.

4. RESULTS

The liquid association point's p stacking affirmed fullerene (C60's) noncovalent functionalization of decreased graphene oxide (rGO). A limited quantity of rGO/isopropanol (IPA) mixture was painstakingly added to the C60/m-xylene mixture for a concise timeframe. Amidst two streaming media, there was an unmistakable, faint green interfacing point that showed how C60 and graphene cross rearing created. In view of the center slant, the rGO in IPA and C60 in m-xylene constantly diffuse from their own responses into the association point between these two liquids. Whenever they run into each other in the interfacial locale via a p association, C60 gathers on the rGO surface. Economically breaking free the association point design will yield adequate fullerene-upgraded rGO for some time in the future.

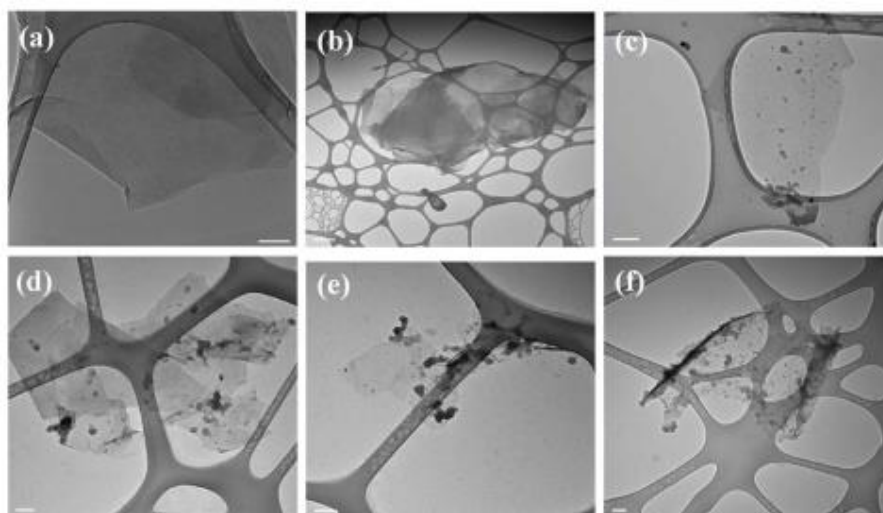


Figure 1: TEM pictures of graphene (a) and the C60/graphene hybrid produced with C60 solution at 0.1, 0.5, 0.75, 1, and 2 mg/ml (b), e, and f. (Bar of scale: 100 nm).

Transmission electron microscopy (TEM) was utilized to portray the as-organized rGO and C60/rGO hybrid, as displayed in Figure 1. There are no apparent particles on the level surface of the rGO. The graphene tests with C60 adornment, which were set up utilizing 0.5, 0.75, 1, and 2 mg/ml C60 game plan, uncover some weak nanoparticles (NPs), which ought to really be C60 bundles. Nonetheless, the C60/rGO cross variety created with 0.1 mg/ml C60 game plan exhibits no C60 nanoparticles on its external layer. This may be the case on the grounds that no NPs were outlined in the wake of adding a subsequent liquid stage since the center point of the C60/m-xylene plan is too little to even consider working with the scattering. Higher centers bring about a get-together at the liquid mark of communication where the fixation point generally drives the scattering. More modest C60 nanoparticles are circular, however bigger nanoparticles, which might frame from the total of little circles, have shifting shapes³¹⁻³⁴. Most surprisingly, the interlayer p association that outlines not many stacked graphene layers causes graphene layers without any trace of C60 molecules to restack (Figure 1b). Nonetheless, the C60/rGO experiments uncovered only one or not very many layered designs, which might be the consequence of the associated C60 particles, which successfully keeps the graphene layers from restacking and amassing together when taken care of in a course of action.

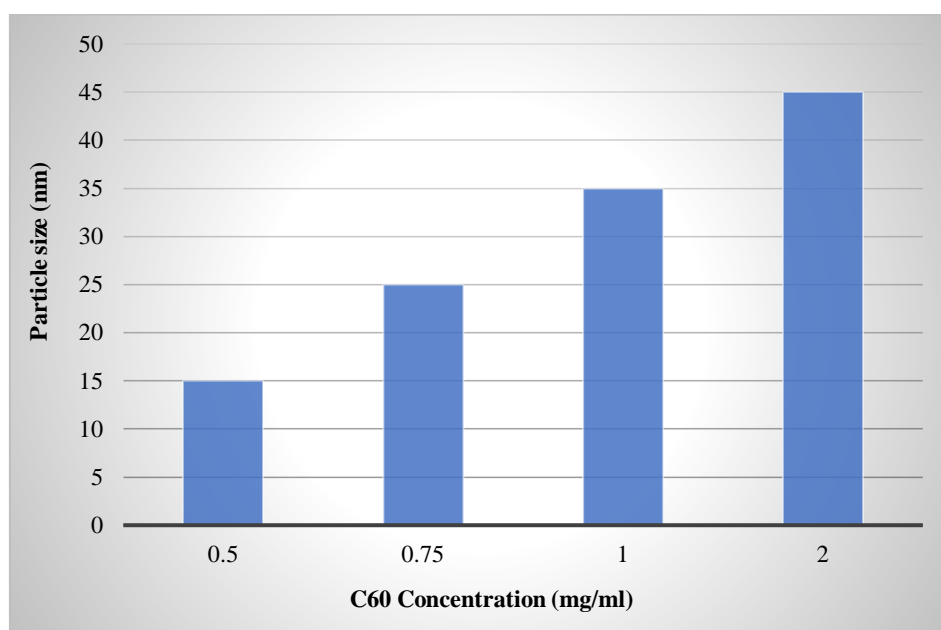


Figure 2: The C60 cluster size at C60/rGO hybrids varies with the starting C60 concentration.

In light of the assessment of C60 gatherings, the particle size scattering of the gathered C60 was dissected and displayed in Figures 2 and S1 (Gainful Materials). The ordinary sub-atomic size at the time a 0.5 mg/ml C60 plan was utilized is 13 nm. Bigger particles are delivered by higher C60 fixations, which arrive at 23, 26, and 32 nm for 0.75, 1 mg/ml, and 2 mg/ml, separately. The bigger particle size ought to be the result of the expanded C60 center, which will by and large shape bigger seeds for the development of nanoparticles. There was no way to see a distinction in the size of C60 nanoparticles when the C60 center was expanded from 0.75 mg/ml to 1 mg/ml in light of the fact that the seed size is essentially affected by the adjustment of C60 fixation from 0.75 to 1 mg/ml. Moreover, contrasted with that made at a lower center, C60-further developed rGO, which was created at a higher C60 fixation, exhibits a more extensive size flow of C60. Fixation exhaustion of the C60 course of action happens after the nucleation at the connection point during the fundamental period of C60 nanoparticle seed development^{35,36}. A C60 fixation tendency was framed inside the interlayer because of the counter dissolvable continuously diffusing into it. This could possibly cause a wide seed size movement. By and large, a higher beginning C60 center will bring about a more remarkable fixation slant and a more extensive size scattering of C60 nanoparticles. It has been noticed that various elements can influence the morphology of nanoparticles, including the stifling extent (against dissolvable/dissolvable volume extents), dissolvable sort, and unfriendly to dissolvable kind. This could give viable method for tending to extra tuning of the C60 nanoparticle size.

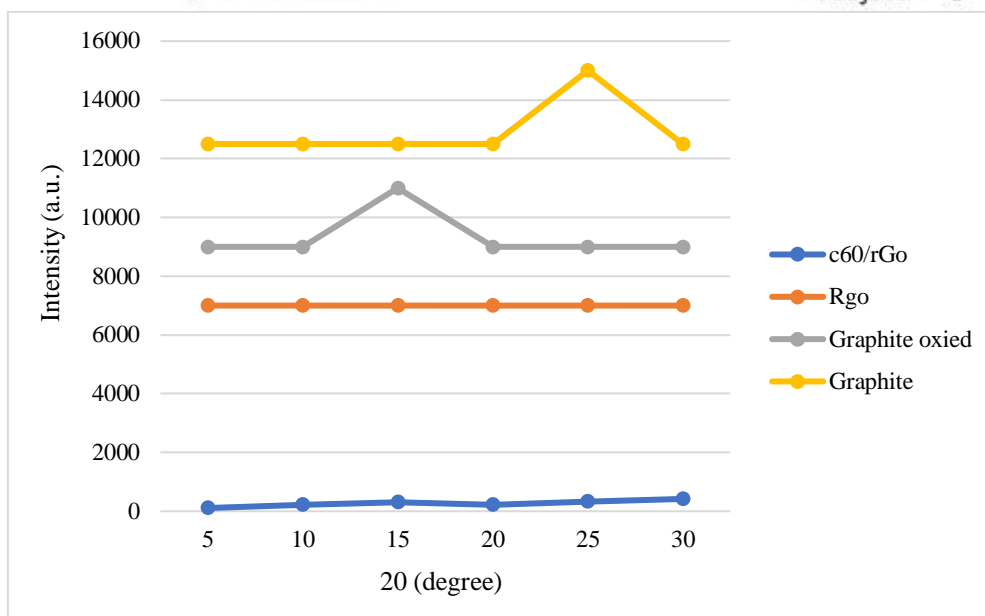


Figure 3: Graphite, graphite oxide, diminished graphene oxide, and C60/rGO half breed XRD designs.

XRD and Raman spectra were utilized to depict the rGO and C60/rGO tests, and they are shown separately in Figures 3 and 4. An interlayer partition of 0.34 nm is found in Figure 3 for ideal graphite at the (002) top at 27u. After oxidization, the (002) apex of graphene oxide (GO) movements to 14.6 u, showing an expansion in interlayer scattering to 0.72 nm³⁸. The intense (002) graphite oxide zenith vanished after manufactured decrease by hydrazine, and a second, more extensive apex, estimating around 24 u, arose. The exfoliation of graphite oxide's layered plans is liable for the sharp pinnacle's vanishing. The expansive pinnacle could be the aftereffect of fractional stacking of foliated graphene sheets. The trademark zeniths of C60 are seen in C60/rGO mixes at 10.8u, 17.7u, 20.8u, 21.7u, 27.5u, and 28.2u corresponding to the C60 diffraction examples of (111), (220), (311), (222), (331), and (420), respectively³⁹. The wide graphene diffraction in the scope of 22u to 26u vanished, and this can be explained by the accumulated C60 bundles, which successfully kept the graphene layers from restacking. The fullerenes had been effectively consolidated onto the external layer of graphene, as exhibited by the X-ray diffraction (XRD) examples, and they filled in as spacers to forestall the individual graphene sheets from restacking.

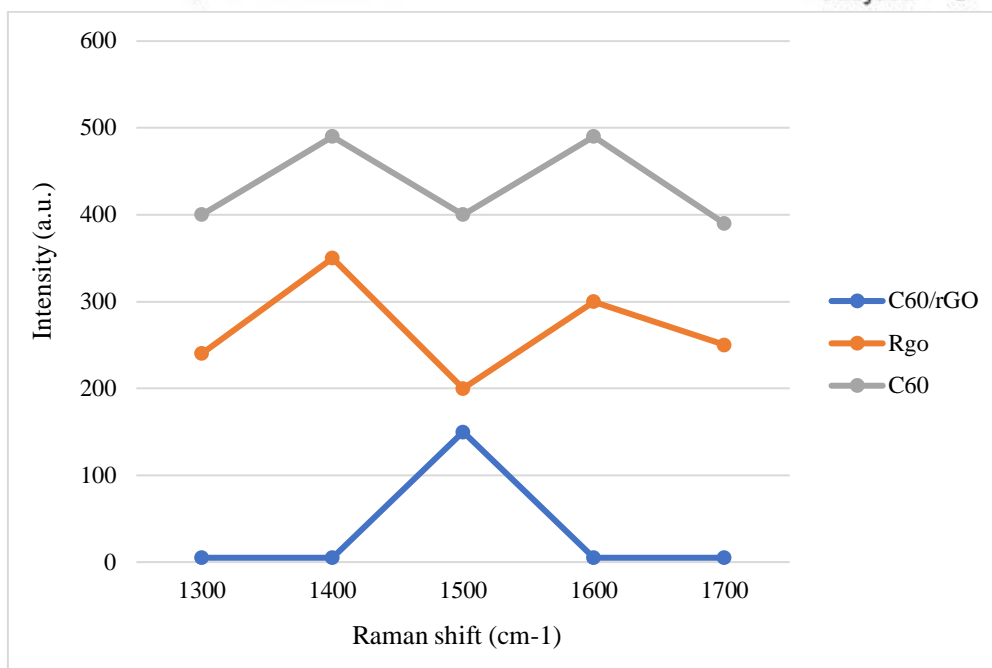


Figure 4:C60, rGO, and C60/rGO crossover Raman spectra.

A fast and non-disastrous strategy for finding out about the electrical and cross-sectional plans of carbon materials is Raman spectroscopy⁴⁰. Figure 4 showed the graphene, impeccable C60, and C60/graphene Raman spectra. A critical G-band (sp² carbon) is found in the rGO at 1576 cm⁻¹, which is equivalent to the E_{g2} phonon in the Brillouin zone's point of convergence. Because of imperfections that were available during the oxidation and lessening procedure⁴², the sp² carbons' out-of-plane breathing component is liable for the D-band (sp³ carbon) at 1348 cm⁻¹. The pentagonal press mode A_g (2) of C60 molecules⁴³ is shown by the sharp top at 1466 cm⁻¹. Three Raman tops were seen at 1344 cm⁻¹, 1467 cm⁻¹, and 1582 cm⁻¹ in the C60/rGO cream. These relate to the D band (1344 cm⁻¹), the G band (1582 cm⁻¹) of graphene, and the pentagonal crush technique for C60 particles (1467 cm⁻¹), separately. Furthermore, in the C60/graphene mixture, the graphene G band (1575 cm⁻¹) upshifts to 1582 cm⁻¹, showing a charge-move from graphene to C60⁴⁴. It is affirmed by the Raman information that C60 were effectively assembled onto graphene and that a charge moves happened among graphene and C60 particles.

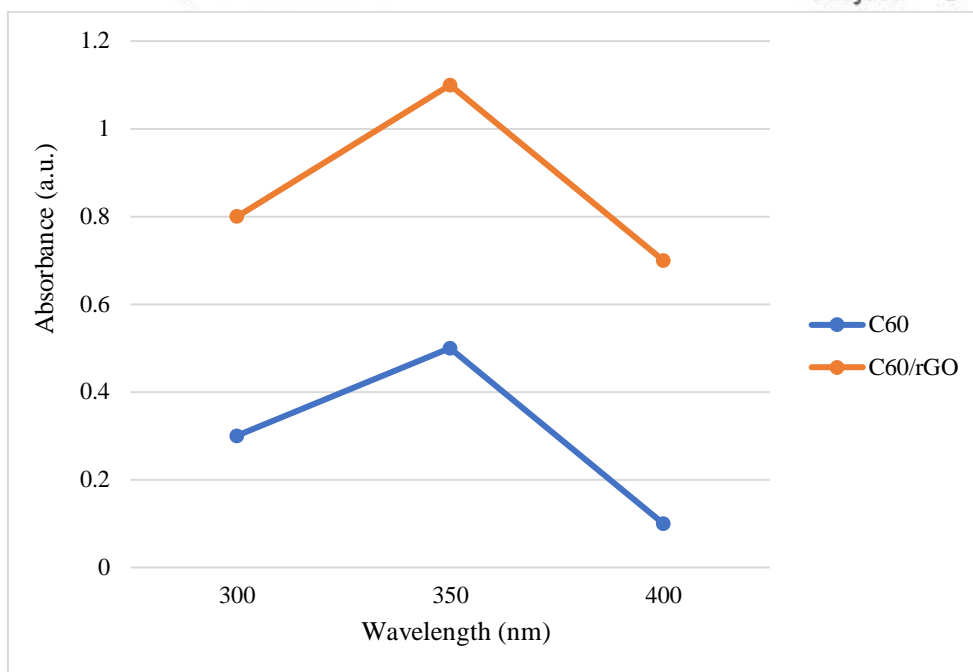


Figure 5: UV-Vis spectra of the in-arrangement C60 and C60/rGO half and half.

By enlightening the C60 and C60/rGO arrangements independently, the UV-Vis spectra of each were acquired. The C60's territory has two unmistakable tops at 280 and 328 nm, as found in Figure 5. The p electronic headways are the wellspring of the top at 328 nm. The red shift of the top at 328 nm is related with the communications among C60 and different particles; subsequently, this pinnacle fills in as a vital pointer for the collaboration of fragrant rings and fullerenes. The p stacking of graphene and C60 might diminish the energy for the electronic transition³² and delocalize the p electron system. The pinnacle of the C60 moves from 328 nm to 334 nm in the C60/rGO, demonstrating that the C60 was effectively accumulated to graphene and that the p association basically works with the development of the C60/rGO cross varieties as expected.

5. DISCUSSION

Despite the fact that graphene has a zero bandgap and is a semi-metallic material, it was found that C60-further developed rGO exhibits a restricted band opening relying upon the level of C60 functionalization. Modified thermoelectric qualities may be accomplished by coordinating as-conveyed nanohybrids into the created polymer (PEDOT: PSS) to change the electrical and phonon transport. The weight stacking of C60-spiced up rGO was fixed at 30%

weight rate in light of the dealing with difficulties and consistency of morphology around then. The impacts of stacking rGO and C60 on the thermoelectric attributes of the subsequent composites were explored. For the C60-further developed rGO/polymer composites, the electrical conductivity, warm conductivity, and Seebeck coefficient were all totally assessed at room temperature.

Figure 6 gave an extra portrayal of the part. Lower rGO weight stacking showed higher C60 weight stacking since the C60/rGO mutt weight stacking in PEDOT: PSS composites was fixed at 30 wt%. The C60 nanoparticles' strong electron scattering will cause them to rethink expanding their electron transportability. Moreover, as was at that point said, C60 and rGO's participation in correspondence exhibited their agreeable relationship. Low electrical conductivity might result from a high electrical contact obstacle brought about by the feeble contact between the cross-breed filler and polymer. Also, the electrical conductivity might be additionally decreased by the massive distinction in electrical conductivity between C60 ($10219-10211 \text{ S/cm}$)²⁵ and rGO, or C60 and PEDOT: PSS polymers. The electrical conductivity of the composite was diminished for a higher measure of C60 because of its high electrical obstruction.

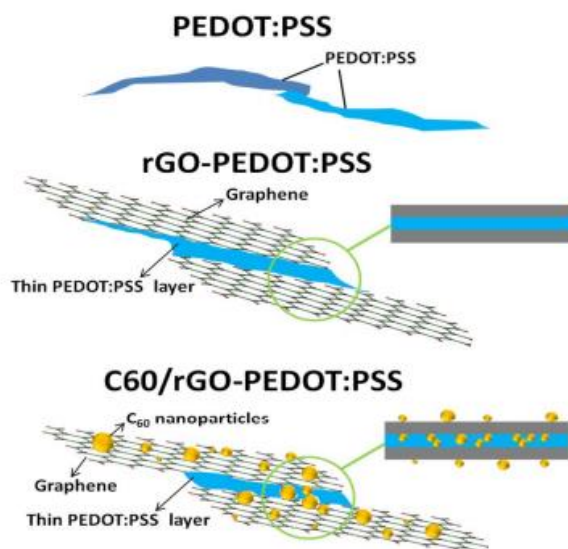


Figure 6: Diagrammatic representation of carrier transport in C60/rGO nanohybrid-filled polymer composites, rGO-polymer, and neat polymer films.

The C60 atom size on graphene surfaces increments from 10 nm to 40 nm, as found in Figure 2. Huge C60 particles diffuse phonons at focus frequencies, little C60 particles diffuse phonons at short frequencies, and slender PEDOT: PSS layers outlined interfaces for long-recurrence phonon scattering between rGO layers. One may hypothetically indicate a normal sans mean methodology for phonons that convey most of the power. In this way, solid phonon scattering will happen as per the Casimir regime when the particle size meets the phonon mean turnpike in PEDOT: PSS. Lower get segment warm conductivity is accomplished through the scattering of phonons with complete frequencies by the C60 nanoparticles on the graphene external layer. Given its hydrophobic part, C60-advanced graphene would without a doubt likewise familiarize penetrability development and further lessen warmed conductivity. It has been noticed that poreable PANI composites increment thermoelectric ZT by diminishing warm conductivity while keeping up with electrical conductivity. Figure 7 shows a SEM picture of the nanohybrid composites at x 5 %. Limited scope pores were seen.

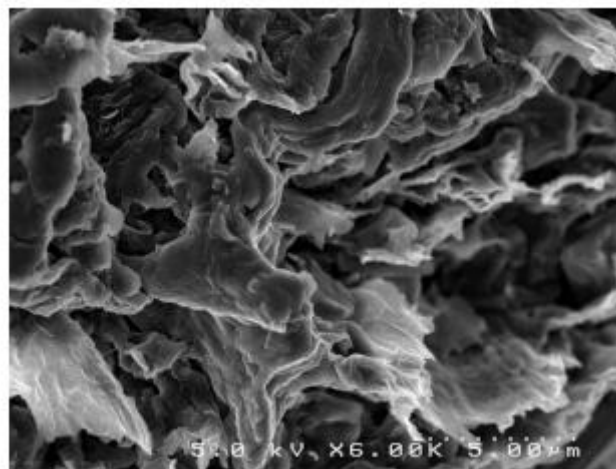


Figure 7:The common microstructure of polymer composites stacked with nanohybrids.

As displayed in Figure 6, the ZT was likewise determined as the ability of x in the rGOxC60302x nanohybrid-filled polymer composites. ZT would by and large increment with x # 21% on the grounds that, as Figures 6 and 8 show, the ascent in electrical conductivity was a lot quicker than the ascent in warm conductivity. ZT would regularly diminish at x = 21% since the composites' warm conductivity expanded essentially and significantly more rapidly than their electric conductivity. Accordingly, in the rGOxC60302x nanohybrid-filled

polymer composites, where the proportion of C60 to rGO was 357, the most noteworthy ZT was accomplished at $ZT = 0.067$ when $x = 21\%$. Thermoelectric properties of graphene/polymer and fullerene/polymer composites were additionally researched independently for relationship, in spite of the fact that their ZT was just 1023. Thus, the joined impacts of graphene and C60 can alleviate the difficulties looked by warm/electric vehicles and result in the biggest ZT in polymer composites.

6. CONCLUSION

Including hierarchical nanostructures may up another road to work on organic composites' thermoelectric performance. The exact control of Nano association, interfacial plan, and dopant melding has permitted researchers to exhibit striking enhancements in these materials' electrical conductivity, Seebeck coefficient, and warm conductivity. Successful administration of hierarchical fullerene-graphene nanohybrids was accomplished, and development portrayals, like TEM, XRD, Raman, and UV-Vis spectra, approved the improvement of fullerene on rGO and the exchange of charge between them. Hence, by adding such new hierarchical nanohybrids into a made polymer, organic thermoelectric materials were created. Because of the conceivable interfacial energy detachment, 4-envelope improvement in the Seebeck coefficient was accomplished in the hierarchical nanohybrid-filled polymer composites when contrasted and the ideal polymer film. The electrical conductivity of the nanohybrids can be tuned to outflank the expansion of warm conductivity by changing the extent of C60 to graphene. This outcomes in an ideal $ZT = 0.067$, which is in excess of a 10-overlay improvement over the single-stage filler-based polymer composites. Integrating a few layered heterogeneous nanomaterial nanohybrids into polymers opens up another road for the development of superior performance organic thermoelectric materials.

REFERENCES

1. Akizu-Gardoki O, Bueno G, Wiedmann T, Lopez-Guede J M, Arto I, Hernandez P and Moran D 2018 Decoupling between human development and energy consumption within footprint accounts *Journal of Cleaner Production* 202 1145-1157

2. Balcilar M, Ozdemir Z A, Ozdemir H and Shahbaz M 2018 *Carbon dioxide emissions, energy consumption and economic growth: The historical decomposition evidence from G-7 countries.*
3. Chu S, Cui Y and Liu N J N m 2017 *The path towards sustainable energy Nature materials* 16 16
4. Du, Y. et al. *Simultaneous increase in conductivity and Seebeck coefficient in a polyaniline/graphene nanosheets thermoelectric nanocomposite. Synth. Met.* 161, 2688–2692 (2012).
5. Duan J, Chen S and Zhao C 2017 *Ultrathin metal-organic framework array for efficient electrocatalytic water splitting Nature communications* 8 15341
6. He C, Wu S, Zhao N, Shi C, Liu E and Li J 2013 *Carbon-encapsulated Fe₃O₄ nanoparticles as a high-rate lithium ion battery anode material ACS nano* 7 4459-69
7. Huang C H, Zhang Q, Chou T C, Chen C M, Su D S and Doong R A 2012 *Three-dimensional hierarchically ordered porous carbons with partially graphitic nanostructures for electrochemical capacitive energy storage ChemSusChem* 5 563-71
8. Kong D, Luo J, Wang Y, Ren W, Yu T, Luo Y, Yang Y and Cheng C 2014 *Three-Dimensional Co₃O₄@ MnO₂ Hierarchical Nanoneedle Arrays: Morphology Control and Electrochemical Energy Storage Advanced Functional Materials* 24 3815-26
9. Mao, A. Q. et al. *Synthesis of graphene oxide sheets decorated by silver nanoparticles in organic phase and their catalytic activity. J. Phys. Chem. Solids.* 73, 982–986 (2012).
10. Muhumuza R, Zacharopoulos A, Mondol J D, Smyth M and Pugsley A 2018 *Energy consumption levels and technical approaches for supporting development of alternative energy technologies for rural sectors of developing countries Renewable and Sustainable Energy Reviews* 97 90-102
11. Roemmich D, Church J, Gilson J, Monselesan D, Sutton P and Wijffels S 2015 *Unabated planetary warming and its ocean structure since 2006 Nature climate change* 5 240
12. Schaffner M, England G, Kolle M, Aizenberg J and Vogel N 2015 *Combining Bottom-Up Self-Assembly with Top- Down Microfabrication to Create Hierarchical Inverse Opals with High Structural Order Small* 11 4334-40
13. Xiang, J. L. & Drzal, L. T. *Templated growth of polyaniline on exfoliated graphene nanoplatelets (GNP) and its thermoelectric properties. Polymer* 53, 4202–4210 (2012).

14. Yang L, Chu D, Wang L, Ge G and Sun H 2016 *Facile synthesis of porous flower-like SrCO₃ nanostructures by integrating bottom-up and top-down routes* *Materials Letters* 167 4-8
15. Zhang Q, Huang J Q, Qian W Z, Zhang Y Y and Wei F 2013 *The road for nanomaterials industry: A review of carbon nanotube production, post-treatment, and bulk applications for composites and energy storage* *Small* 9 1237-65

Author's Declaration

I as an author of the above research paper/article, hereby, declare that the content of this paper is prepared by me and if any person having copyright issue or patent or anything otherwise related to the content, I shall always be legally responsible for any issue. For the reason of invisibility of my research paper on the website/amendments/updates, I have resubmitted my paper for publication on the same date. If any data or information given by me is not correct, I shall always be legally responsible. With my whole responsibility legally and formally have intimated the publisher (Publisher) that my paper has been checked by my guide (if any) or expert to make it sure that paper is technically right and there is no unaccepted plagiarism and hentriconane is genuinely mine. If any issue arises related to Plagiarism/ Guide Name/ Educational Qualification/ Designation/ Address of my university/ college/institution/ Structure or Formatting/ Resubmission /Submission /Copyright /Patent/Submission for any higher degree or Job/Primary Data/Secondary Data Issues. I will be solely/entirely responsible for any legal issues. I have been informed that the most of the data from the website is invisible or shuffled or vanished from the database due to some technical fault or hacking and therefore the process of resubmission is there for the scholars/students who finds trouble in getting their paper on the website. At the time of resubmission of my paper I take all the legal and formal responsibilities, If I hide or do not submit the copy of my original documents(Andhra/Driving License/Any Identity Proof and Photo) in spite of demand from the publisher then my paper maybe rejected or removed from the website anytime and may not be consider for verification. I accept the fact that As the content of this paper and the resubmission legal responsibilities and reasons are only mine then the Publisher (Airo International Journal/Airo National Research Journal) is never responsible. I also declare that if publisher finds Any complication or error or anything hidden or implemented otherwise, my paper maybe removed from the website or the watermark of remark/actuality maybe mentioned on my paper. Even if anything is found illegal publisher may also take legal action against me

Mahesh Kumar Chandna
Dr. Vivek Yadav